

Photoclinic

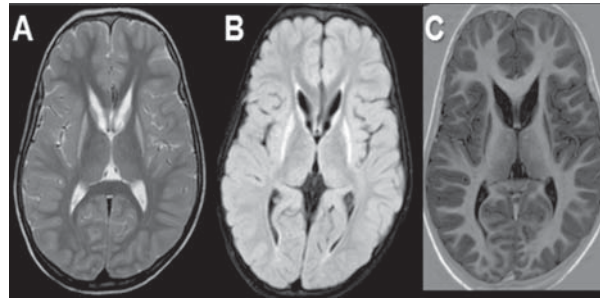


Figure 1. T2 weighted axial (A) and FLAIR axial (B) images show symmetric hyperintensity involving the caudate nucleus and putamen on both sides. Axial T1 inversion recovery (IR) image (C) shows marked atrophy of the caudate nuclei and putamina.

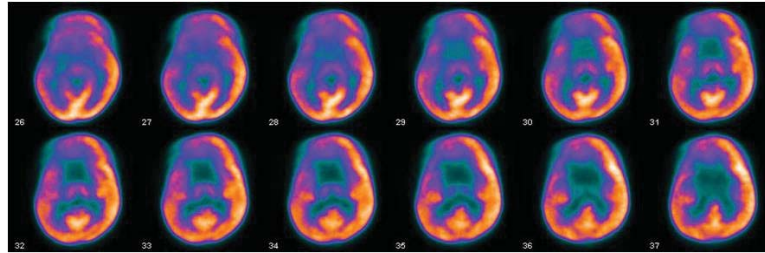


Figure 2. FDG PET images reveal symmetric striatal hypometabolism. An area of hypometabolism seen on attenuated corrected images in the right frontal region is due to motion artefact.

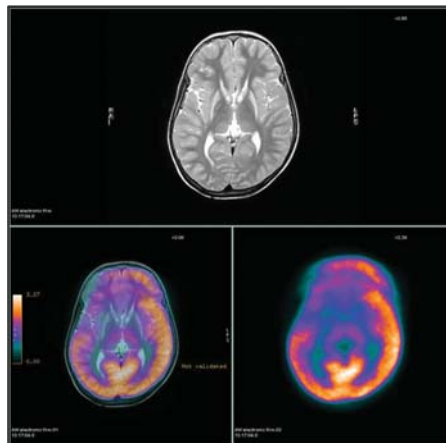


Figure 3. Fused images of FDG PET and T2 weighted axial images reveal hypometabolism in the atrophic caudate nuclei and putamina.

Cite the article as: Naphade PS, Keraliya AR, Shah HJ, Lele VR. Photoclinic. *Arch Iran Med.* 2013; **16(10)**: 611 – 612.

A 9-year-old male child presented to our institute with a history of cognitive decline, seizures, imbalance, and frequent falls since two years. The birth history was unremarkable. The family history was remarkable with patient’s uncle having abnormal movements and psychiatric symptoms. Blood counts were unremarkable. Magnetic resonance imaging (MRI) of the brain revealed symmetric T2/ fluid attenuated inversion recovery (FLAIR) hyperintensity involving the caudate nucleus and putamen on both sides. There was a marked atrophy of the caudate nucleus and putamen

on both sides with resultant enlargement of the frontal horns of lateral ventricles (Figure 1). The globus pallidus and the cerebellum were not involved. We injected 5 mci of 18F-fluorodeoxyglucose (FDG) and scanned the patient after two hours. Positron emission tomography/computed tomography (PET/CT) was acquired on GE Discovery 16-slice PET/CT in dedicated brain PET protocol. There was presence of a severe hypometabolism in the striatum (Figures 2 and 3). An additional area of hypometabolism was seen on attenuated corrected images in the right frontal region due to motion artefact; this was not appreciated on nonattenuation corrected images. Rest of the brain parenchyma showed normal metabolism.

Prashant S. Naphade MD¹, Abhishek R. Keraliya DNB¹, Hina J. Shah DNB², Vikram R. Lele DNB²

Authors’ affiliations: ¹Department of Radiology, ESIC Hospital, Mumbai-400093, India. ²Department of Nuclear Medicine, Jaslok Hospital, Mumbai-400026, India.

Corresponding author and reprints: Prashant S. Naphade MD DNB, Department of Radiology, ESIC Hospital, Andheri East, Mumbai-400093, India. Tel: +91-9920914963, E-mail: prashant.nafade@gmail.com.

Accepted for publication: 21 August 2013

**What is your diagnosis?
See the next page for diagnosis.**

Huntington disease (HD) is a progressive neurodegenerative disorder with autosomal dominance inheritance pattern. The disease is a trinucleotide repeat disorder caused by high instability and extension of CAG sequences within the coding region of IT15 gene. Juvenile HD with an age of onset before 20 years is less common than adult-onset HD. The common presenting symptoms of juvenile HD are dystonia, rigidity, bradykinesia, declining cognitive function, seizures, and behavioral disturbances. Chorea which is a prominent feature of adult-onset HD is a very uncommon presenting symptom of juvenile HD, which may occur during the course of the disease.

The main radiologic feature of juvenile HD is atrophy of neostriatum consisting of the caudate nucleus and putamen. On T2 and FLAIR images, these structures display hyperintense signal. Selective neuronal loss involving the caudate nucleus and putamen with gliosis explains the signal abnormalities. Frontal horns enlargement is seen due to the caudate head atrophy. The caudate atrophy can be quantified by a decrease in the frontal horn width to intercaudate distance ratio (FH/CC), or intercaudate distance to inner table width ratio (CC/IT). These measurements are taken on axial images at the level of the third ventricle. The normal mean FH/CC ratio range is 2.2 to 2.6. The normal CC/IT ratio range is 0.09 to 0.12.¹ In addition to the above-mentioned changes, there may be involvement of the globus pallidus and the cerebellum in juvenile HD. Diffuse cerebral atrophy is also seen.

Glucose metabolism in the brain predominantly occurs in astrocytes, thus astrocyte dysfunction or death results in selective impairment of cerebral glycolysis; this may result in the loss of their ability to protect neurons, and raises the likelihood that such dysfunction may be a crucial step in the pathogenesis of HD. 18F-FDG is a PET tracer which demonstrates the glucose metabolism

abnormalities. In HD, there is a reduction of glucose metabolism seen in striatum; this finding has been demonstrated in many studies.^{2,3}

The differential diagnoses of symmetrical involvement of the basal ganglia as in HD include Leigh disease, Wilson disease, carbon monoxide poisoning, acute hypoxia, and hypoglycemic encephalopathy. Majority of these conditions can be differentiated from juvenile HD on clinical grounds. In Wilson disease and Leigh disease additional involvement of subcortical white matter, thalamus, brain stem, and cerebellum is seen which is not seen in HD.^{4,5}

Striatal atrophy on MRI and striatal hypometabolism on FDG PET are useful imaging to confirm clinical diagnosis of juvenile HD.

References

1. Barr AN, Heinze WJ, Dobben GD, Valvassori GE, Sugar O. Bicaudate index in computerized tomography of Huntington disease and cerebral atrophy. *Neurology*. 1978; **28**: 1196 – 1200.
2. Kuhl DE, Phelps ME, Markham CH, Metter EJ, Riege WH, Winter J. Cerebral metabolism and atrophy in Huntington's disease determined by 18FDG and computed tomographic scan. *Ann Neurol*. 1982; **12**: 425 – 434.
3. Kuwert T, Lange HW, Langen KJ, Herzog H, Aulich A, Feinendegen LE. Cortical and subcortical glucose consumption measured by PET in patients with Huntington's disease. *Brain*. 1990; **113**: 1405 – 1423.
4. Hegde AN, Mohan S, Lath N, Lim CC. Differential diagnosis for bilateral abnormalities of the basal ganglia and thalamus. *Radiographics*. 2011; **31**: 5 – 30.
5. Comunale JP Jr, Heier LA, Chutorian AM. Juvenile form of Huntington's disease: MR imaging appearance. *AJR Am J Roentgenol*. 1995; **165**: 414 – 415.